15th Triennial World Congress, Barcelona, Spain

ON THE SLIDING MODE CONTROL FOR DC SERVO MECHANISM IN THE PRESENCE OF UNMODELED DYNAMICS

Jian-Xin Xu*, Ya-Jun Pan* and Tong-Heng Lee*

* *Electrical and Computer Engineering Department*
National University of Singapore, Singapore,117576
Email: `elexujx@nus.edu.sg`

Abstract: In this paper, via describing function techniques, sliding mode control of DC servo mechanisms is analyzed in the presence of unmodeled dynamics. We first show that, a conventional sliding mode controller with signum function will inevitably generate a limit cycle where a second or higher order unmodeled dynamics exists. A fractional interpolation based smoothing scheme is then proposed to eliminate the limit cycle, and maintain a reasonable tracking precision bound. In particular, a DC servo motor with unmodeled stator and sensor dynamics is taken into consideration. Both theoretical analysis and simulation results verify the effectiveness of the proposed new fractional interpolation control scheme.

Keywords: Sliding Mode Control, Unmodeled Dynamics, Describing Function, Limit Cycle, Smoothing Control.

1. INTRODUCTION

It is well known that Variable Structure Control (VSC) with sliding mode has superior robustness to matched system uncertainties (Utkin, 1992) (Young and Ozguner, 1993) (Xu *et al.*, 1997) (Man and Yu, 1997) (Xu *et al.*, 2000). However, such a SMC may lose its robustness when unmodeled system dynamics exist, as the discontinuous switching will lead to limit cycles – the chattering phenomenon.

There are two factors jointly generating a limit cycle: a relative degree above two and an overhigh control gain around the equilibrium. According to classical control theory, a higher relative degree implies the possibility of a large phase lag beyond $-180°$. Meanwhile a higher gain means a less phase margin. Unfortunately, a typical discontinuous switching control in SMC possesses an infinite gain in the equilibrium. When the system is strictly positive real (relative degree one), a phase margin of $90°$ is guaranteed. Limit cycles occur mainly in two circumstances: either in the presence of a sampling delay or an unmodeled dynamics of relative degree above two.

Let us first look at the sampling delay. Since a sampling mechanism generates a pure time delay, the corresponding Nyquist curve will move spirally towards the origin and cut cross the negative real axis infinitely many times. Thus at certain phase cross frequency the phase reaches $-180°$ and limit cycles occur. As far as a servo system is concerned, with a perfect switching mechanism (infinite switching frequency available or equivalently the sampling delay is infinitesimal), phase crossover frequency is also infinity and the limit cycle magnitude is zero owing to the low pass filter nature of the servo. In practice when the sampling frequency is limited, a common way to eliminate chattering is to incorporate a smoothing control scheme to reduce the gain around the equilibrium.

In the presence of unmodeled dynamics, the chattering problem will be worsened due to the extra phase lag, thereafter a rather lower phase crossover frequency and a larger chattering magnitude. In particular when the unmodeled part has a relative degree of two or above, limit cycles are inevitable even with a perfect switching mechanism. Most SMC designs for servomechanism ignore two kinds of dynamic factors in the motor stator circuit and sensor devices (encoder and tachogenerator). They will present at least two first order low pass filters cascaded to the mechanical part of the servomechanism.

Here a question is, can we take those dynamic factors into consideration in SMC design? The first difficulty we have is the availability of internal state variables corresponding to those unmodeled dynamics. The second difficulty is the presence of unknown parameters in unmodeled dynamics, which hinders state estimation. Third, by taking stator dynamics, encoder and tachogenerator dynamics into account, the system is of fifth order (likely higher with state estimation), and the sliding mode controller would be over complicated for practical servo applications. On the other hand, the unmodeled dynamics are stable and usually less influential to matched disturbance rejection. Thus we can extend the widely adopted chattering elimination approach – smoothing the control input. Note that this way leads to a lower control gain in servo mechanisms, consequently to certain extent sacrifices control precision. However this will be rewarded by the elimination of limit cycles that usually generate a larger tracking error and lead to fast wear and tear of torque transmission device. Moreover, the SMC can be designed solely based on the reduced order servo system, i.e. the mechanical part without concerning the unmodeled dynamics.

In this work, a new fractional interpolation based smoothing scheme is proposed to eliminate the limit cycle in DC servo mechanisms. Because of the nonlinear switching control in SMC, the describing function method, an extended version of the frequency response method for linear systems (Slotine and Li, 1991), is used to analyze and predict the limit cycle approximately. Through both theoretical analysis and simulation of a typical DC servo mechanism, it is verified that the limit cycle occurs if a conventional SMC with signum function is applied, and disappears when the SMC is revised with an appropriate smoothing scheme.

The paper is organized as follows. Section 2 gives the descriptions of the DC servo motor and the unmodeled dynamics. In Section 3, via describing function techniques, the limit cycle problem associated with SMC is first analyzed, then a new smoothing function is introduced to eliminate limit cycles. Section 4 considers a DC servo motor and shows the validity of the analysis and the effectiveness of the proposed control scheme.

2. PROBLEM FORMULATION

A. Mechanical Dynamics of DC Servo

A typical DC servo motor can be expressed as below

$$J\ddot{\theta} + b_s\dot{\theta} + k_s\theta = \tau + \tau_l \tag{1}$$

where θ is the motor angular displacement, τ and τ_l are the motor torque and load torque respectively, J is the total inertia, b_s is the viscous friction coefficient and k_s is the spring constant. Defining $x_1(t) = \theta$ and $x_2(t) = \dot{\theta}$, the state space form of (1) is

$$\begin{cases} \dot{x}_1(t) = x_2(t), \\ \dot{x}_2(t) = -\dfrac{1}{J}(k_s x_1 + b_s x_2) + \dfrac{1}{J}(\tau + \tau_l) \end{cases} \tag{2}$$

where $x_1(0) = \theta(0)$ and $x_2(0) = \dot{\theta}(0)$. Note that (1) or (2) represents the mechanical subsystem of the DC servo. Often the sliding surface is designed by taking this mechanical subsystem into account, which is $\sigma = e_2 + c_1 e_1$ where $e_1 = x_1 - x_{d,1}$, $e_2 = x_2$ and $x_{d,1}$ is a set point. The simplest switching control is $\tau = -k\ sign(\sigma)$, where the gain k is designed appropriately by taking all servo system uncertainties into account. A convenient design tool is the Lyapunov's direct method with the Lyapunov function candidate $V = \frac{1}{2}\sigma^2$. It is worthy to point out that the relative degree from the system input τ to the extended output σ is one. Hence the process is may have a phase margin of 90°

B. Unmodeled Dynamics

In practice the DC servo motor has a first order stator electrical dynamics

$$\begin{aligned} \dot{I}_q &= \frac{1}{L_q}(u - RI_q), \\ \tau &= k_t I_q, \end{aligned} \tag{3}$$

where I_q is the q-axis current, L_q is the q-axis inductance, R is the stator resistance, u is the control input voltage and k_t is the torque constant. Define a new state $x_3(t) = I_q$, (3) becomes

$$\dot{x}_3 = \frac{1}{L_q}(u - Rx_3), \tag{4}$$

and its transfer function is

$$D_1(s) = \frac{\tau(s)}{u(s)} = \frac{\frac{k_t}{L_q}}{s + \frac{R}{L_q}}. \quad (5)$$

Another source of unmodeled dynamics is related to sensing devices. A sensor is truly a dynamic system and the general dynamic structure of a sensor is (Bernstein, 2001)

$$\dot{z} = f(z, x), \qquad \hat{x} = \phi(z, x), \quad (6)$$

where z is the internal sensor state, x is the physical input to the sensor, and $\hat{x}$ is the sensor output. In the DC servo motor, the angular displacement x_1 is measured by encoder and the angular velocity x_2 by tachogenerator. By considering the sensor dynamics, we have the following relationship

$$\tau_1\dot{\hat{x}}_1 + \hat{x}_1 = k_1 x_1, \qquad \tau_2\dot{\hat{x}}_2 + \hat{x}_2 = k_2 x_2,$$

where $\hat{x}_1$ and $\hat{x}_2$ are the acquired state variables through sensor dynamics. In practice the sensor DC gains k_1 and k_2 can be easily calibrated through static tests. However it is not an easy task to accurately measure time constants τ_1 and τ_2.

The transfer function from the applied switching surface $\hat{\sigma}$ to the theoretical one is

$$D_2(s) = \frac{\hat{\sigma}(s)}{\sigma(s)} = \frac{\frac{k_2 s}{\tau_2 s+1} + \frac{c_1 k_1}{\tau_1 s+1}}{s + c_1} = \frac{\tau_1 k_2 s^2 + (k_2 + c_1 k_1 \tau_2)s + c_1 k_1}{[\tau_1\tau_2 s^2 + (\tau_1 + \tau_2)s + 1]\,(s + c_1)}. \quad (7)$$

Remark 1: *It is a common practice to use low pass filters to get rid of measurement noise. In such case τ_1 and τ_2 should include these filter time constants. In addition, there often exist a variety of parasitic dynamics in practical systems and they also account for the existence of unmodeled dynamics.*

Due to the existence of above two classes of unmodeled dynamics, the system may not work properly under a conventional sliding mode scheme with signum function, or even under a smoothing control scheme. This can be shown in the analysis of the subsequent sections via describing function techniques.

3. DESCRIBING FUNCTION TECHNIQUES BASED ANALYSIS

A. Limit Cycle Problem with Signum Function

The system in (1) can be rewritten as an extended error dynamics

$$\begin{cases} \dot{e}_1(t) = e_2(t), \\ \dot{e}_2(t) = -a_0 e_1 - a_1 e_2 - a_0 e_3 + b\tau \\ \dot{e}_3(t) = 0 \end{cases} \quad (8)$$

where $a_0 = k_s/J$, $a_1 = b_s/J$, $b = 1/J$ and $e_3(t) = x_{d,1}$ is a constant. The switching control with signum function is $\tau = -k\ sign(\sigma)$. The block diagram of the system is shown in $Fig.1$, where $G(s)$ can be regarded as a low pass filter without poles at the origin

$$G(s) = \frac{\sigma(s)}{\tau(s)} = \frac{b(s + c_1)}{s^2 + a_1 s + a_0}. \quad (9)$$

Define $G_d(s) = D_1(s)G(s)D_2(s)$ which is the transfer function of the plant linear part.

Assume there exists a self-sustained oscillation (limit cycle) of amplitude A_c and frequency ω_c. When ω_c is sufficiently high in comparison with the cut-off frequency of $G_d(j\omega_c)$, according to the describing function analysis method the switching surface can be approximately written as $\sigma = A_c sin(\omega_c t)$. Limit cycles exist if the Nyquist curve of the linear plant $G_d(j\omega_c)$ intersects with $H(A, \omega) = -1/N(A, \omega)$, where $N(A, \omega)$ is the describing function of the system nonlinear part. The describing function of the signum function is $N(A) = 4k/\pi A$. Thus $H(A, \omega) = -1/N(A)$ is the whole negative real axis with the initial point $(0, 0)$ corresponding to $A = 0$.

There will be three possible classes of system motions in terms of the intersection points as shown in $Fig.2$. In the absence of unmodeled dynamics D_1 and D_2, since the relative degree of $G(s)$ in (9) is one, there is an intersection at $(A_c = 0 \cup \omega_c = \infty)$. This is exactly the ideal sliding motion which has infinite switching frequency and zero off-set. Owing to the theoretically larger phase margin (90°), any extra small phase lag practically existing, such as sampling delay, will produce a limit cycle with very small magnitude. Next when the system linear part has relative degree two, i.e. either GD_1 or GD_2 is under consideration, the intersection point is still at $(A_c = 0 \cup \omega_c = \infty)$. However, the phase margin in this case could be zero, which implies that the system may not be robust at all. Hence the extra small phase lag may produce limit cycle with relatively large magnitude. Finally, if a second order unmodeled dynamics D_1D_2 is present, there definitely exists one intersection at $(A_c > 0 \cup \omega_c < \infty)$, thereby limit cycle motion exists even without considering any extra phase lag factors.

B. Limit Cycle Elimination with a New Fractional Interpolation Smoothing Control Scheme

In order to eliminate the limit cycle problem described above, a new fractional interpolation smoothing control scheme below is proposed to replace the signum function

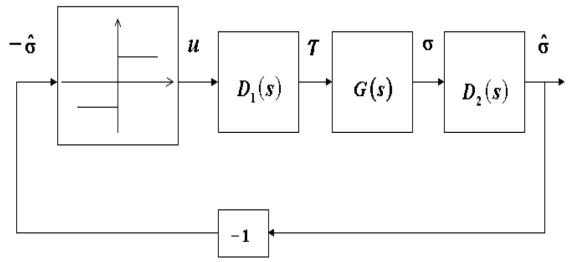

Fig. 1. Block diagram of the DC servo motor with signum function.

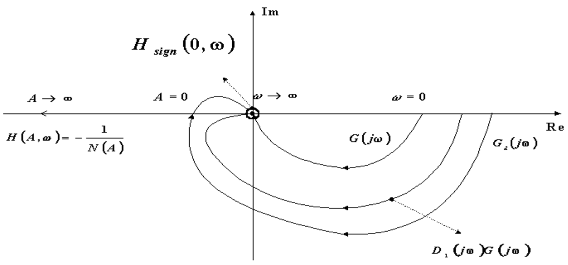

Fig. 2. Detections of the limit cycle in the DC servo motor.

$$u = -k\ \frac{(|\sigma| + \delta_1)\sigma}{(|\sigma| + \delta)^2} = -k_e\ sign(\sigma), \quad (10)$$

where the equivalent switching gain is

$$k_e = k\ \frac{(|\sigma| + \delta_1)|\sigma|}{(|\sigma| + \delta)^2},$$

and δ and δ_1 are two design parameters.

Proposition: *The proposed control law (10) with* $\delta_1 = 2\delta + \frac{\delta^2}{\eta}$, *where* η *is a prespecified tracking precision bound, ensures the following three properties.* $P1^\circ$ *The equivalent control gain* $k_e \geq k$ *when* $|\sigma| \geq \eta$, *which means the equivalent gain is adequate outside the precision bound.* $P2^\circ$ *The switching control* u *is continuously differentiable with respect to* σ *(smoothness property).* $P3^\circ$ *The equivalent switching control gain* $k_e \Rightarrow k$ *as* $|\sigma| \Rightarrow \infty$, *i.e. maintains at a moderate level.*

The new fractional interpolation smoothing scheme is able to eliminate limit cycles, as given in the following theorem.

Theorem: *The Nyquist plot of* $H(A,\omega) = -\frac{1}{N(A)}$, *where* $N(A)$ *is the describing function of the proposed controller, will be a line on the negative real axis from the initial point* $(-\frac{\delta\eta}{k(2\eta+\delta)}, 0)$ *to the end point* $(-\infty, 0)$.

Proof: See *Appendix*. ■

Let γ be the maximum value of the magnitude of $|G_d(j\omega)|$ at the phase crossover frequency ω_{pc}, i.e. the leftmost point m in *Fig*.3, while the unmodeled dynamics D_1 and D_2 take all possible values. By properly selecting the parameters δ and η such that $\delta\eta / [k(2\eta + \delta)] > \gamma$, we can achieve the sliding mode without any limit cycle.

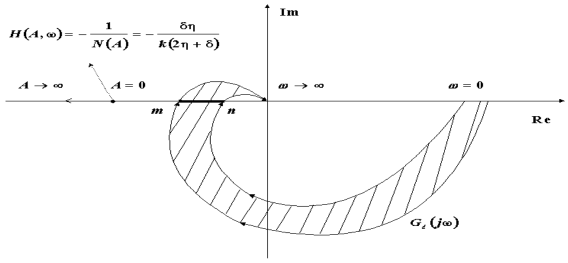

Fig. 3. Detection of a limit cycle in the case of a second order unmodeled dynamics.

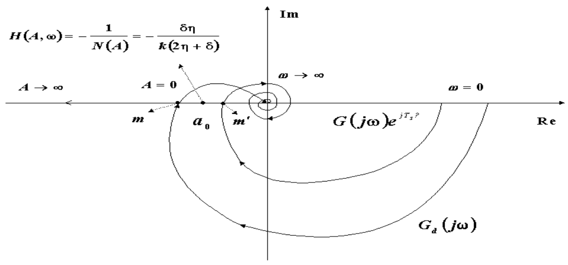

Fig. 4. Detection of a limit cycle in the case of a second order unmodeled dynamics and sampling delay.

Remark 2: *A sampled-data system with limited sampling frequency will inevitably incur a pure time delay* e^{-sT_s} *with the sampling period* T_s. *Fig*.4 *shows that the Nyquist plot of system* $G(s)e^{-sT_s}$ *approaches the origin in a spiral manner, hence there are theoretically infinite intersections with the negative real axis, therefore infinite number of limite cycles. Usually in practical systems the sampling period is sufficiently small, thus the* m' *point, which corresponds to the limit cycle with the maximum magnitude, will be very near to the origin. This implies that limit cycles due to sampling delay can be easily avoided by introducing a smoothing function which moves the rightmost point of* $H(0,\omega)$ *from origin to the position* a_0. *Note that a small* η *can achieve this if* a_0 *is small. As a consequence, a small* T_s *allows a higher precision bound. It can also be seen from* *Fig*.4 *that, to avoid the point* m *we have to further move* a_0 *leftwards, leading to a rather larger* η – *a lower tracking precision.*

4. AN ILLUSTRATIVE EXAMPLE WITH DC SERVO MOTOR

Consider the DC servo motor dynamics described by (1), (3) and (7) jointly. The parameters are $J = 6.0 \times 10^{-2}\ Kg \cdot m$, $k_s = 0.255\ N \cdot m/rad$, $b_s = 0.075\ N \cdot m \cdot sec/rad$, $L_q = 11.6 \times 10^{-3}\ H$, $R = 2.215\ \Omega$, $k_t = 1$, $\tau_1 = 0.01$, $\tau_2 = 0.008\ sec$ and $k_1 = k_2 = 1$. The set point is $\theta_d = 2\ rad$. The sampling interval is $T_s = 0.001\ sec$. The sliding surface is $\sigma = e_2 + 6e_1$. The initial values of the states are $x_1(0) = 1$ and $x_2(0) = -1$. The initial values of unmodeled dynamics are assumed to be zero. The switching control gain can be calculated as $k = 5.3$. $G(s)$ in (9), $D_1(s)$ and $D_2(s)$ are

$$G(s) = \frac{16.67(s+6)}{s^2 + 1.25s + 4.25}, D_1(s) = \frac{86.2}{s + 190.93}$$
$$D_2(s) = \frac{125s^2 + 12585s + 75000}{(s^2 + 225s + 12500)(s+6)}.$$

The prior knowledge of the unmodeled dynamics is that the parameters L_q, R, k_t, τ_1 and τ_2 vary $\pm 20\%$ from their rated values.

Case 1: No Unmodeled Dynamics

First look at the SMC with signum function. As shown in $Fig.5$, there exists a very small limit cycle in the absence of unmodeled dynamics. This limit cycle is due to sampling delay and can be easily eliminated by the smoothing scheme (10) with the tracking precision bound $\eta = 0.08$ ($\delta = 1$), see $Fig.6$.

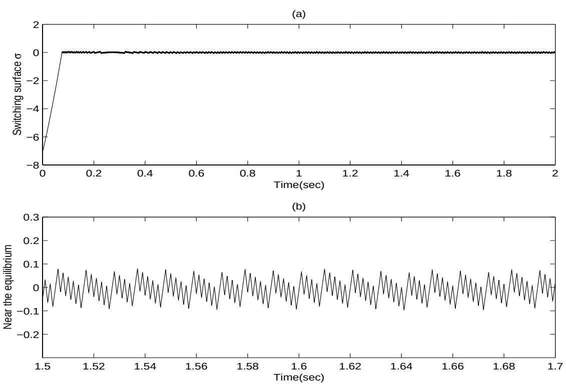

Fig. 5. System performance under conventional signum controller without unmodeled dynamics: (a) Switching surface; (b) Near the equilibrium.

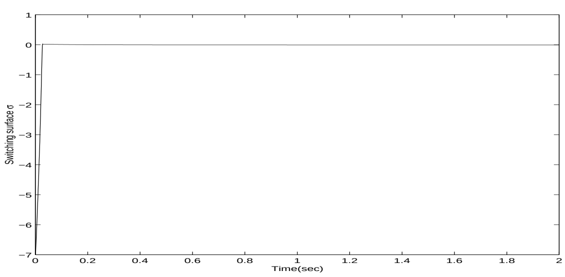

Fig. 6. The evolution of the switching surface under the proposed fractional interpolation scheme ($\eta = 0.08$ and $\delta = 1$).

Case 2: With Unmodeled Dynamics

Now still using the same smoothing control parameters $\eta = 0.08$ ($\delta = 1$), we can see from $Fig.7$ that limit cycle occurs again. By drawing Nyquist plot of $G_d = GD_1D_2$ and taking the $\pm 20\%$ parametric variations into account, we can see that the two extreme points are at m (-0.034) and n (-0.0176) as shown in $Fig.8$. On the other hand, $H(0, \infty) = -\frac{\delta\eta}{k(2\eta+\delta)} = -0.013$ falls even right to the n point, thus the limit cycle is inevitable, and incurs rather larger tracking error $\sigma \approx 0.8$.

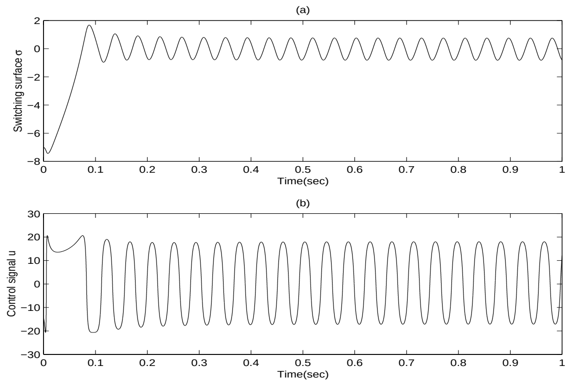

Fig. 7. System performance under the proposed fractional interpolation control scheme ($\eta = 0.08$ and $\delta = 1$) with the second order stable unmodeled dynamics $D_1(s)D_2(s)$: (a) Switching surface; (b) Control profile.

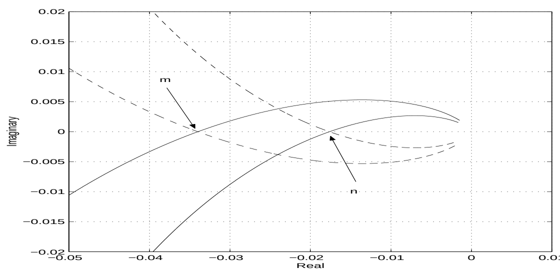

Fig. 8. The nyquist plot of the system $G_d(s) = D_1(s)G(s)D_2(s)$.

Finally to eliminate limit cycle we have to further reduce the control gain with $\eta = 0.3$, $\delta = 1.5$. Now $H(0, \omega) = -\frac{\delta\eta}{k(2\eta+\delta)} = -0.04$ which is again left to m. We are able to produce very smooth control responses and smooth control input profiles shown in $Fig.9$. The actual error at steady state is 0.049, which is far lower than the preceding circumstance.

5. CONCLUSIONS

In this paper, describing function techniques are applied to analyze the sliding mode control of the DC servo mechanisms. In the presence of unmodeled dynamics, especially when the unmodeled part has a relative degree of two or above, the limit cycle problem will happen when using conventional SMC scheme with switching mechanism. The proposed new fractional interpolation smoothing scheme, which is used to avoid high switching chattering, effectively eliminate the limit cycle. Moreover, the new smoothing scheme can be easily designed based on the reduced order servo mechanical system.

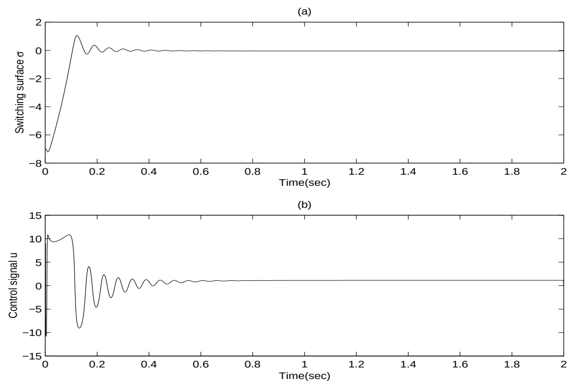

Fig. 9. System performance with proposed controller ($\eta = 0.3$ and $\delta = 1.5$) in the case of the second order stable unmodeled dynamics: (a) Switching surface; (b) Control profile.

REFERENCES

Bernstein, D.S. (2001). Sensor performance specifications. *IEEE Control Systems Magazine* **21**, 9–18.

Man, Z. and X.H. Yu (1997). Terminal sliding mode control of MIMO linear systems. *IEEE Transactions on Circuits and Systems I: Fundamental Theory and Applications* **44**, 1065–1070.

Slotine, J.J.E. and W.P. Li (1991). *Applied nonlinear control.* PH. Englewood Cliffs, New Jersey.

Utkin, V.I. (1992). *Sliding Modes in Control and Optimization.* Springer-Verlag. Berlin.

Xu, J.X., Q.W. Jia and T.H. Lee (2000). Adaptive robust control schemes for a class of nonlinear uncertain descriptor systems. *IEEE Transactions on Circuits and Systems I: Fundamental Theory and Applications* **47**, 957–962.

Xu, J.X., T.H. Lee and C. He (1997). Controller design for a class of nonlinear multi-input systems using modified sliding mode. *International Journal of Systems Science* **28**, 777–789.

Young, K.D. and U. Ozguner (1993). Frequency shaping compensator design for sliding mode. *International Journal of Control* **57**, 1005–1019.

APPENDIX: PROOF OF $THEOREM$.

Consider the input of the control function (10) is $-\sigma = Asin(\omega t)$, then the output is

$$u(t) = \frac{k[|Asin(\omega t)| + \delta_1]Asin(\omega t)}{[|Asin(\omega t)| + \delta]^2}. \quad (11)$$

Define $r = Asin(\omega t)$ for simplicity. In case of $A \leq \delta$, (11) can be expressed by series expansion

$$u(t) = \frac{k(|r| + \delta_1)r}{(|r| + \delta)^2} = -\frac{k(|r| + \delta_1)r}{\delta}\frac{d}{d|r|}\left(\frac{1}{1 + \frac{|r|}{\delta}}\right)$$

$$= \sum_{i=1}^{i=\infty}(-1)^{i+1}\frac{[i\delta_1 - (i-1)\delta]\,kr|r|^{i-1}}{\delta^{i+1}}$$

$$= \sum_{i=1}^{i=\infty} h_i, \quad (12)$$

where $h_i = (-1)^{i+1}\frac{[i\delta_1 - (i-1)\delta]kr|r|^{i-1}}{\delta^{i+1}}$. The output in (11) can be expanded as a Fourier series, with the fundamental being

$$u_1 = \bar{a}_1 cos(\omega t) + \bar{b}_1 sin(\omega t).$$

Because $u(t)$ is an odd function with respect to σ, $\bar{a}_1 = 0$. The coefficient $\bar{b}_1$ is

$$\bar{b}_1 = \frac{1}{\pi}\int_{-\pi}^{\pi}\sum_{j=1}^{j=\infty} h_j sin(\omega t)d\omega t = \sum_{j=1}^{j=\infty} b_j. \quad (13)$$

The integrations of the first three parts are $b_1 = \frac{Ak\delta_1}{\delta^2}$, $b_2 = -\frac{2A^2k(2\delta_1-\delta)}{\pi\delta^3}$ and $b_3 = \frac{A^3k(3\delta_1-2\delta)}{4\delta^4}$. From (12), it is easy to know that the jth ($j > 3$) parts left in (13) will be $b_j = A^j d_j$, $j > 3$, where d_j is the coefficient composed of the parameters k, δ_1 and δ. Then

$$\bar{b}_1 = \frac{Ak\delta_1}{\delta^2} - \frac{2A^2k(2\delta_1 - \delta)}{\pi\delta^3} + \frac{A^3k(3\delta_1 - 2\delta)}{4\delta^4} + \sum_{j=4}^{\infty} A^j d_j.$$

Therefore, when $A \leq \delta$ is satisfied, the describing function of the proposed control scheme is

$$N(A) = \frac{\bar{b}_1}{A} = \frac{k\delta_1}{\delta^2} - \frac{2Ak(2\delta_1 - \delta)}{\pi\delta^3} + \frac{A^2k(3\delta_1 - 2\delta)}{4\delta^4} + \sum_{j=4}^{\infty} A^{j-1}d_j.$$

$$H(A,\omega)\mid_{A=0} = -\frac{1}{N(A)}\mid_{A=0} = -\frac{\delta\eta}{k(2\eta + \delta)}.$$

From (13), $H(A,\omega)$ can also be expressed as

$$H(A,\omega) = -\frac{1}{N(A)} = -\frac{A}{\bar{b}_1} = -\frac{\pi}{4k\int_0^{\frac{\pi}{2}} v(A,\omega t)d\omega t},$$

where $v(A,\omega t) = \frac{[|Asin(\omega t)| + \delta_1]sin^2(\omega t)}{[|Asin(\omega t)| + \delta]^2}$. $\forall A_1 > 0$, $v(A_1,\omega t) < v(0,\omega)$ because

$$v(A_1,\omega t) - v(0,\omega t) = -\frac{sin(\omega t)^2|A_1 sin(\omega t)|}{\delta^2\left[|A_1 sin(\omega t)| + \delta^2\right]^2} \cdot\left[(2\delta + \frac{\delta^2}{\eta})|A_1 sin(\omega t)| + (3\delta^2 + \frac{2\delta^2}{\eta})\right] < 0.$$

Then $\forall A \in (0,\infty)$, $H(A,\omega) < H(0,\omega) = -\frac{\delta\eta}{k(2\eta+\delta)} < 0$.